Imaging of dislocations in β-Ga_2O_3 via X-ray topography based on anomalous transmission

β-Ga_2O_3 is a promising ultrawide bandgap semiconductor suitable for use in high-voltage and high-current power electronics applications [1]. Single-crystal substrates with highly crystalline structures are a prerequisite for guaranteeing high-performance and reliable β-Ga_2O_3 devices. Although high-quality and large-diameter (~10 cm) bulk crystals are now commercially available [2], a further reduction in crystallographic defects is required. A major type of crystallographic defect in β-Ga_2O_3 that limits device performance is dislocations present at the densities of 10^3–10^5 cm^{-2}. The knowledge of their character and distribution over an entire crystal volume is of considerable scientific and industrial importance. However, this knowledge has not been available for β-Ga_2O_3 owing to the lack of available techniques to probe dislocations located in the deep interiors of thick crystals.

In this study, we performed a transmission XRT observation at SPring-8 **BL24XU** to reveal the dislocation distribution over the entire volume of a large β-Ga_2O_3 substrate [3,4]. This technique takes advantage of the anomalous transmission (AT) of X-rays, which is a dynamical diffraction phenomenon known as the Borrmann effect [4]. The sample was a Sn-doped (001)-oriented β-Ga_2O_3 single-crystal substrate fabricated via edge-defined film-fed growth (EFG). The rectangular substrate had the dimensions of 10 mm × 15 mm and a thickness of 680 μm. Monochromatic X-rays of wavelength λ = 1.24 Å were used to irradiate the sample, which had a μt value of approximately 9.7 at this wavelength, where μ is the linear absorption coefficient and t is the sample thickness. A forward-diffracted beam (o-wave) was used for imaging.

Figure 1(a) shows a schematic of the substrate geometry and optical system using the diffraction vector $\boldsymbol{g}$ = 020. X-rays entered the sample from one of the (001) surfaces, and the exiting X-rays were first irradiated onto a vertically movable fluorescent screen (FS). The occurrence of AT was determined by observing the spot intensity on the FS, which corresponded to the o-wave and h-wave (diffracted beam). According to the theoretical description of AT using dynamical XRD theory, the two plane waves are coherently coupled in the crystal, and their interference produces a set of standing waves. When the zero-amplitude points (nodes) of standing waves coincide with the atomic planes used for Bragg reflection, the intensity of the photoelectric absorption is significantly reduced, leading to a marked increase in the intensity of the transmitted X-rays [5]. Figures 1(b,c) show the photographs of the o- and h-wave spots on the FS under normal absorption and AT conditions at $\boldsymbol{g}$ = 020, respectively. There was a 180 arcsec difference in the ω angle of the two conditions. Under normal absorption, a significant attenuation caused by the large value of μt (~9.7) led to a faint o-wave spot, and the h-wave spot was not recognizable (Fig. 1(b)). In comparison, when the ω angle was carefully adjusted to satisfy the exact Bragg condition of $\boldsymbol{g}$ = 020, which allowed AT to occur, two equally strong spots corresponding to the o- and h-waves were observed (Fig. 1(c)). Figures 1(d,e) show the photographs of $\boldsymbol{g}$ = 022 under similar conditions. After two equally strong spots were confirmed, the FS was moved upward to allow the o-wave to advance toward the camera for image recording.

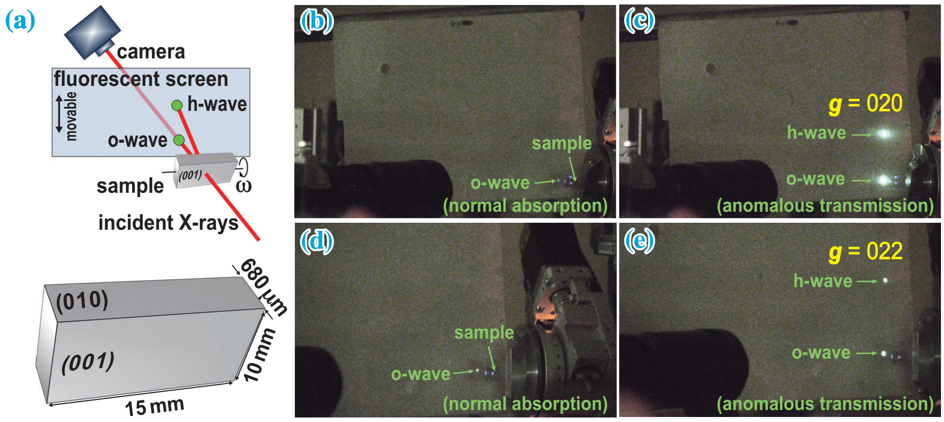

Fig. 1. **(a)** Schematic of the substrate geometry and the optical system; **(b)–(e)** photographs of the o- and h-wave spots on the FS under normal absorption or anomalous transmission conditions.

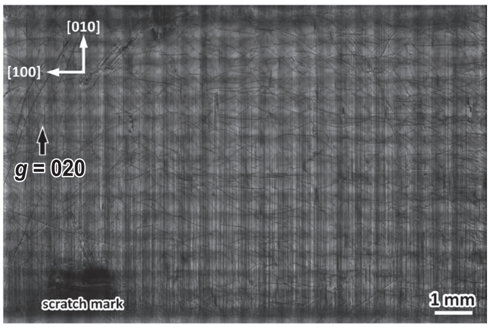

Fig. 2. BF-XRT of the entire sample obtained with $\boldsymbol{g}$ = 020.

Figure 2 shows the BF-XRT results for the entire sample obtained at $\boldsymbol{g}$ = 020. Dislocations having a Burgers vector $\boldsymbol{b}$ = [uvw], with $v \neq 0$, were revealed. The dominant feature of the topograph is highly dense vertical lines. The vast majority of them corresponded to dislocations parallel to the [010] direction, indicating that threading dislocations in the [010] direction were the most stable and frequently generated dislocations during EFG. In comparison, the curved lines had a lower density, and most were associated with dislocations lying on the (001) plane. Dynamical XRD theory predicts that dislocations close to the exit surface generate a sharper contrast than those close to the entrance surface. Therefore, the degree of sharpness of the curved lines indicated the depth of the dislocations from the (001) surfaces.

To identify the character of the dislocations, that is, their Burgers vectors, transmission XRTs of the same area were acquired at $\boldsymbol{g}$ = 022 and $\boldsymbol{g}$ = 400. A comparison between $\boldsymbol{g}$ = 020 and $\boldsymbol{g}$ = 022 (Fig. 3) reveals a significant number of additional vertical lines that are not observed in Fig. 2. Judging by the $\boldsymbol{g}\cdot\boldsymbol{b}$ invisibility criterion, these dislocations must have a Burgers vector of $\boldsymbol{b}$||[001], presumably $\boldsymbol{b}$ = [001] (or $\boldsymbol{b}$ = [$00\bar{1}$]). A remarkable feature of the 400 topograph is the complete extinction of all curved dislocations, indicating that these dislocations have a Burgers vector of the form $\boldsymbol{b}$ = [$0vw$], that is, they possess no a-axis components. Moreover, the curving feature strongly suggests that they were not generated via dislocation propagation in the [010] direction during EFG pulling-up, but were highly likely to have been generated via dislocation glide on the (001) plane under thermal stress. To glide on the (001) plane, w in $\boldsymbol{b}$ = [$0vw$] must be zero. Therefore, we conclude that all the curved dislocations share the same Burgers vector $\boldsymbol{b}$ = [010] (or $\boldsymbol{b}$ = [$0\bar{1}0$]) and that the glide belongs to the [010](001) slip system.

Table I. Dislocation visibility at various $\boldsymbol{g}$-vectors and the corresponding dislocation type

Label	$\boldsymbol{g}$			$\boldsymbol{b}$	ξ	Type
	020	022	400			
1	Yes	Yes	Yes	N/A	N/A	Macro defects
2	Yes	Yes	No	[010]	[010]	b-axis screw
3	No	Yes	No	[001]	[010]	b-axis edge
4	Yes	Yes	No	[010]	curved, ∈(001)	Mixed type
5	No	Yes	Yes	[$u0w$], likely [$10\bar{1}$]	roughly [010]	Edge

(Yes = visible; No = invisible; N/A = not applicable).

The dislocation visibilities and corresponding dislocation types are listed in Table I. Thus, we successfully revealed the dislocation distribution and dislocation characters for a large-area β-Ga_2O_3 substrate. The transmission XRT technique based on AT is a powerful tool for imaging dislocations in highly absorbing β-Ga_2O_3, which can provide important feedback for the improvement of crystal growth.

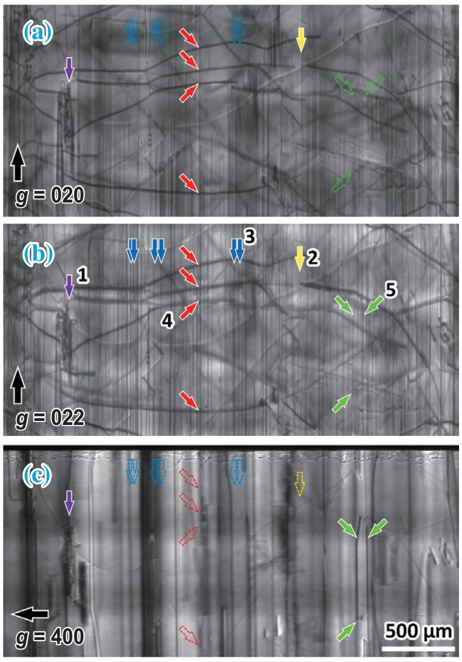

Fig. 3. Comparison of dislocation visibility among: **(a)** $\boldsymbol{g}$ = 020; **(b)** $\boldsymbol{g}$ = 022; and **(c)** $\boldsymbol{g}$ = 400. The scale bar applies to all images.

Yongzhao Yao[†]

Functional Materials Group, Japan Fine Ceramics Center

Email: y_yao@jfcc.or.jp

[†] Present address: Mie University

References

[1] S. Pearton *et al.*: Appl. Phys. Rev. **5** (2018) 011301.
[2] A. Kuramata *et al.*: Jpn. J. Appl. Phys. **55** (2016) 1202A2.
[3] Y. Yao *et al.*: APL Mater. **10** (2022) 051101.
[4] *Y. Yao, Y. Tsusaka, K. Sasaki, A. Kuramata, Y. Sugawara and Y. Ishikawa: Appl. Phys. Lett.* ***121*** *(2022) 012105.*
[5] G. Borrmann: Z. Phys. **127** (1950) 297.